# Redox Buffer Capacity of Ion-Selective Electrode Solid Contacts Doped with Organometallic Complexes

Xue V. Zhen, Celeste R. Rousseau, and Philippe Bühlmann\*

Department of Chemistry, University of Minnesota, 207 Pleasant St. SE, Minneapolis, MN 55455, United States

#### **ABSTRACT**

While ion-selective electrodes (ISEs) with inner filling solutions are used widely, solidcontact ISEs are better suited for miniaturization and mass manufacturing. Calibration-free measurements with such electrodes require the reproducible control of the phase boundary potential between the ion-selective membrane and the underlying electron conductor. The most promising approach to achieve this goal is based on redox buffers incorporated into the ionselective membrane. Here we introduce the theory and present experimental data for Co(III), Co(II), Ru(II), Fe(II), and Os(II) compounds that show quantitatively how the phase boundary potential at a solid contact doped with redox-active compounds is affected by weighing errors, reagent impurities, and redox-active interferents. Perhaps surprisingly, theory predicts that there is only a minimal dependence of the phase boundary potential on the ratio of the concentrations of a pure oxidized and a pure reduced compounds if those two compounds are not a redox couple. However, theory predicts that even small redox-active impurities of those compounds shift the phase boundary potential drastically. Experimentally, a surprisingly good in-batch reproducibility was observed by us and others for solid contacts prepared to contain either only the reduced or only the oxidized species of a redox couple. This can be explained by redoxactive impurities and is unlikely to be repeatable when different suppliers of reagents are used or long-term experiments are performed. This work confirms that the preferred approach to calibration-free sensing is based on redox buffers that comprise the reduced and oxidized species of a redox couple in well-controlled concentrations.

# **INTRODUCTION**

Ion-selective electrodes (ISEs)<sup>1,2</sup> with ionophore-doped polymeric sensing membranes are used annually for billions of ion measurements and dominate ion analysis in clinical chemistry.<sup>1</sup> In the conventional ISE setup, the sensing membrane separates the sample from an inner filling solution, into which an inner reference electrode is immersed. While widely used, this setup is difficult to miniaturize, hindering both the development of wearable and miniaturizable devices as well as the fabrication of inexpensive ion sensors for point-of-care tests and healthcare in countries with limited resources.<sup>10,10</sup> ISEs with an inner filling solution are also difficult to sterilize,<sup>11</sup> and transmembrane ion fluxes<sup>12</sup> must be carefully controlled to achieve low detection limits. This has resulted in a lot of interest in the development of solid-contact ISEs without an inner filling solution.<sup>12,10,16</sup> Early attempts to directly deposit the ion-selective membrane onto a metal in the form of so-called coated-wire electrodes<sup>17</sup> suffered from device-to-device irreproducibility, drifting potentials in long-term measurements, and all too often device failure due to delamination of the sensor membrane from the underlying electron conductor.

Until recently, the most common approach to address these problems was the use of a conducting polymer to separate the ion-selective membrane from the underlying electron conductor.<sup>18-22</sup> Much progress was made to make these conducting polymers hydrophobic and insensitive to light. Notwithstanding, solid contacts based on conducting polymers that show very low potential drifts in long-term experiments and are characterized by a high device-to-device reproducibility of the calibration curve are still elusive. An interesting alternative to conducting polymers are solid contacts made of nanostructured high-capacity carbon materials or metals.<sup>23-25</sup> In particular, solid contact ISEs that comprise a layer of three-dimensionally ordered macroporous carbon,<sup>30-28</sup> carbon nanotubes,<sup>20-30</sup> colloid-imprinted mesoporous carbon,<sup>30-20</sup> carbon

black,<sup>33</sup> or graphene<sup>34-36</sup> between the ion-selective membrane and the underlying metal conductor were shown to exhibit exceptionally low potential drifts in long-term experiments. However, while such sensors often show a much higher device-to-device reproducibility of the calibration curve than coated-wire ISEs, they must still be calibrated individually.

The calibration-free use of ISEs with high device-to-device reproducibility and very low long-term drift requires the control of the phase boundary potential<sup>37</sup> between the ion-selective membrane and the underlying substrate. In the case of intercalation compounds as that substrate, this is achieved by the presence of the primary ion both in the ion-selective membrane and in the substrate. 38.39 When the underlying substrate is an electron conductor, control of the phase boundary potential can be achieved by use of a well-defined redox couple. For example, silver wires were used as the underlying electron conductor, coated with an ion-selective membrane that comprised a Ag<sup>+</sup> ionophore.<sup>40</sup> This approach works well for Ag<sup>+</sup> ISEs, but it has not been possible to extend it to ISEs with selectivities for other ions because in highly selective ISEs the Ag<sup>+</sup> ions end up being displaced by primary ions for which those ISE exhibits a higher selectivity. This problem can be avoided if the phase boundary potential at the interface of the ion-selective membrane and the underlying electron conductor is controlled by a redox-active organometallic complex present both in its oxidized and reduced form. In this case, the redox couple controls the phase boundary potential to the underlying electron conductor as predicted by the Nernst equation. In the first examples for this approach, tris(phenanthroline) and tris(bipyridyl) complexes of Co(III) and Co(II) were used, resulting in device-to-device reproducibilities as small as 1 mV.41-43

A drawback of using the reduced and oxidized species of a redox couple is that at least one of the two species has an electrical charge and, therefore, may be lost into the sample solution as

the result of ion exchange with the primary ion of the ISE. The more selective an ISE is, the more pronounced this problem becomes.<sup>2</sup> A method to avoid this ion exchange is the covalent attachment of the redox-active species to a polymer, particle, or the electron conductor. To this end, it is very intriguing that Jaworska and co-workers reported a device-to-device reproducibility on the order of 1 mV for ISEs comprising a solid contact based on Co(III) and Co(II) complexes. Importantly, in that work, the Co(III) and Co(II) metals were used in the form of corrole and porphyrin complexes, respectively. As a result, both complexes were electrically neutral, minimizing the loss of these redox-active components into the aqueous phase and diminishing concomitant drift in the emf response. However, because the Co(III) corrole / Co(II) porphyrin pair is not a redox couple, the Nernst equation cannot be used in a direct manner to predict the phase boundary potential at the interface of the ion-selective membrane and the underlying electron conductor. Therefore, while the reported favorable characteristics of those sensors are not in question, it has been unclear why the Co(III) corrole / Co(II) porphyrin system performed as well as it did. To address this conundrum comprehensively, this contribution presents the theory and experimental data that show quantitatively how a solid contact doped with redox-active compounds is affected by weighing and dispensing errors, impurities of the reagents, and redox-active interferents. To add to the data on the Co(III) corrole / Co(II) porphyrin system, we experimentally explored the performance of ISEs with solid contacts doped with a lipophilic Co(III) tris(bipyridine) complex and either Fe(II), Os(II), or Ru(II) tris(bipyridine). We then compared their characteristics theoretically and experimentally to those of ISEs with a solid contact based on a well-defined redox couple.

# **THEORY**

Solid contact layers doped with two redox-active compounds that do not form a redox couple share a number of similarities with redox titrations. However, the two types of systems also differ diametrically, as will be shown in the following. In both cases, two redox equilibria are involved:

$$\mathbf{1}_{\mathrm{ox}} + n_{1} \, \mathrm{e}^{-} \quad \square \qquad \mathbf{1}_{\mathrm{red}} \tag{1}$$

$$\mathbf{2}_{\text{ox}} + n_2 \, \mathbf{e}^- \quad \mathbf{\square} \qquad \mathbf{2}_{\text{red}} \tag{2}$$

where 1 and 2 represent two redox-active species, the subscripts ox and red designate the oxidation state, and  $n_1$  and  $n_2$  are the numbers of electrons required to convert  $\mathbf{1}_{ox}$  and  $\mathbf{2}_{ox}$  to their respective reduced species. In both types of systems,  $\mathbf{2}_{ox}$  may oxidize  $\mathbf{1}_{red}$  if the electron transfer rate is sufficiently large:

$$n_2 \mathbf{1}_{red} + n_1 \mathbf{2}_{ox} = n_2 \mathbf{1}_{ox} + n_1 \mathbf{2}_{red}$$
 (3)

Importantly, in a redox titration, the standard redox potential of  $\mathbf{2}$ ,  $E_2^{\circ}$ , is chosen to be much more positive than  $E_1^{\circ}$ . This ensures that the equilibrium described by eq 3 strongly favors  $\mathbf{1}_{ox}$  and  $\mathbf{2}_{red}$  over  $\mathbf{1}_{red}$  and  $\mathbf{2}_{ox}$ . In stark contrast, in the case of a solid contact layer doped with  $\mathbf{1}_{red}$  and  $\mathbf{2}_{ox}$  as described by Jaworska and co-workers, the equilibrium described by eq 3 lies far to the left. For example, if  $n_1$  and  $n_2$  are both unity,  $\mathbf{1}_{red}$  and  $\mathbf{2}_{ox}$  are chosen to be both 10 mM, and  $E_2^{\circ}$  and  $E_1^{\circ}$  differ by 400 mV, the equilibrium concentrations of  $\mathbf{1}_{ox}$  and  $\mathbf{2}_{red}$  are only 0.004 mM. (The equations to show this are derived below.)

In view of calibration-free potentiometric devices, the most important feature of a solid contact layer prepared to contain  $\mathbf{1}_{red}$  and  $\mathbf{2}_{ox}$  is the extent to which inaccuracies in the concentrations of  $\mathbf{1}_{red}$ ,  $\mathbf{2}_{ox}$ ,  $\mathbf{1}_{ox}$ , and  $\mathbf{2}_{red}$  affect the phase boundary potential,  $\Delta \Phi_{mem,e.c.}$ , at the

Such inaccuracies have two main causes. On one hand, weighing errors may affect the concentrations of  $\mathbf{1}_{red}$  and  $\mathbf{2}_{ox}$ . On the other hand,  $\mathbf{1}_{red}$  and  $\mathbf{2}_{ox}$  may contain impurities of  $\mathbf{1}_{ox}$  and  $\mathbf{2}_{red}$ . Alternatively, other redox-active impurity species introduced unintentionally may react with  $\mathbf{1}_{red}$  and  $\mathbf{2}_{ox}$  to give  $\mathbf{1}_{ox}$  and  $\mathbf{2}_{red}$ , respectively. Because  $\Delta \Phi_{mem,e.c.}$  is included as an additive term in the cell potential of an ion-selective device (see, e.g., Fig. 9 in ref. 6 or Fig. 1 in ref. 13),<sup>4-6</sup> the concentrations of  $\mathbf{1}_{red}$ ,  $\mathbf{2}_{ox}$ ,  $\mathbf{1}_{ox}$ , and  $\mathbf{2}_{red}$  directly affect the reproducibility of the y-axis intercept of the calibration curve of solid contact ISEs. Inaccuracies in the concentrations of these species in freshly prepared devices determine whether a device can be considered calibration-free for a particular application. Moreover, how frequently a device needs to be recalibrated depends on the extent to which the concentrations of  $\mathbf{1}_{red}$ ,  $\mathbf{2}_{ox}$ ,  $\mathbf{1}_{ox}$ , and  $\mathbf{2}_{red}$  change over time as a result of (i) losses of these compounds into samples and (ii) their reaction with redox-active components of measured samples. In the following, the effects of small changes in the concentrations of  $\mathbf{1}_{red}$ ,  $\mathbf{2}_{ox}$ ,  $\mathbf{1}_{ox}$ , and  $\mathbf{2}_{red}$  on  $\Delta \Phi_{mem,e,c.}$  are discussed.

Let us first consider the effect of concentration inaccuracies in systems prepared from  $\mathbf{1}_{red}$  and  $\mathbf{2}_{ox}$  prepared from reagents that contain neither impurities of  $\mathbf{1}_{ox}$  and  $\mathbf{2}_{red}$  nor redox-active compounds that can react with  $\mathbf{1}_{red}$  and  $\mathbf{2}_{ox}$  to give  $\mathbf{1}_{ox}$  and  $\mathbf{2}_{red}$ . Inaccuracies in the concentrations of such a system may arise form weighing or dispensing errors during the preparation of the ion-selective membranes, or contamination of the reagents  $\mathbf{1}_{red}$  and  $\mathbf{2}_{ox}$  with inert compounds, limiting the purity of these compounds. In such as system, the only source of  $\mathbf{1}_{ox}$  and  $\mathbf{2}_{red}$  is the redox reaction described by eq 3. It follows that

$$[\mathbf{1}_{ox}] = [\mathbf{2}_{red}] \tag{4}$$

where the square brackets refer to the concentrations of the respective species. Assuming for

simplicity that  $n_1$  and  $n_2$  are unity, the equilibrium constant for eq 3 is

$$K = ([\mathbf{1}_{ox}] [\mathbf{2}_{red}]) / ([\mathbf{1}_{red}] [\mathbf{2}_{ox}])$$

$$(5)$$

and insertion of (4) into (5), followed by solving for  $[1_{ox}]$ , gives

$$[\mathbf{1}_{ox}] = (K [\mathbf{1}_{red}] [\mathbf{2}_{ox}])^{1/2}$$

$$(6)$$

To determine the value of K, the Nernst equation is formulated for 1 and for 2:

$$\Delta \Phi_{\text{mem,e.c.}} = E_1^{\circ} - R T F^{-1} \ln \left( \left[ \mathbf{1}_{\text{red}} \right] / \left[ \mathbf{1}_{\text{ox}} \right] \right)$$
 (7)

$$\Delta \Phi_{\text{mem,e.c.}} = E_2^{\circ} - R T F^{-1} \ln ([\mathbf{2}_{\text{red}}] / [\mathbf{2}_{\text{ox}}])$$
 (8)

where R, T, and F are the universal gas constant, temperature, and Faraday constant, respectively. Since **1** and **2** are in redox equilibrium with one another, the right hand sides of eqs 7 and 8 can be set equal to each other.

$$E_1^{\circ} - R T F^{-1} \ln ([\mathbf{1}_{red}] / [\mathbf{1}_{ox}]) = E_2^{\circ} - R T F^{-1} \ln ([\mathbf{2}_{red}] / [\mathbf{2}_{ox}])$$
 (9)

which can be rearranged to give

$$-F(E_1^{\circ} - E_2^{\circ})/(RT) = \ln(([\mathbf{1}_{ox}] [\mathbf{2}_{red}])/([\mathbf{1}_{red}] [\mathbf{2}_{ox}]))$$
(10)

From eq 5 it follows that the right hand side of eq 10 equals  $\ln K$ . Insertion of  $[\mathbf{1}_{ox}]$  from eq 6 and K from eq 10 into eq 7 lets us calculate  $\Delta \Phi_{\text{mem,e.c.}}$  for a system prepared with  $\mathbf{1}_{red}$  and  $\mathbf{2}_{ox}$  only.

$$\Delta \Phi_{\text{mem,e.c.}} = E_1^{\circ} + R T F^{-1} \ln \left( K^{1/2} \left[ \mathbf{2}_{\text{ox}} \right]^{1/2} / \left[ \mathbf{1}_{\text{red}} \right]^{1/2} \right)$$
 (11)

For illustration, Panel A of Figure 1 shows with the *solid* curve  $\Delta \Phi_{\text{mem,e.c.}}$ , as computed for a system in which [ $\mathbf{1}_{\text{total}}$ ] is constant, and [ $\mathbf{2}_{\text{total}}$ ] is varied from 0 to 300 mol % with respect to [ $\mathbf{1}_{\text{total}}$ ]. Because it was assumed for this plot that  $E_1^{\circ} - E_2^{\circ} = 400 \text{ mV}$ , the concentrations [ $\mathbf{1}_{\text{ox}}$ ] and [ $\mathbf{2}_{\text{red}}$ ] are extremely small, and the total concentrations of  $\mathbf{1}$  and  $\mathbf{2}$ , i.e., [ $\mathbf{1}_{\text{total}}$ ] and [ $\mathbf{2}_{\text{total}}$ ], are approximately equal to [ $\mathbf{1}_{\text{red}}$ ] and [ $\mathbf{2}_{\text{ox}}$ ], respectively. This is illustrated by Panel B of Figure 1.

As evident from Figure 1A, theory predicts, for a system prepared from  $\mathbf{1}_{red}$  and  $\mathbf{2}_{ox}$  only, a

minimal dependence of  $\Delta \Phi_{\text{mem,e.c.}}$  on the ratio of  $[\mathbf{2}_{\text{ox}}]$  and  $[\mathbf{1}_{\text{red}}]$ . This can be readily understood considering eq 11, which for a constant value of  $[\mathbf{1}_{\text{red}}]$  allows for inclusion of the  $[\mathbf{1}_{\text{red}}]$  term into a modified  $E_1^{\circ\circ}$ , simplifying eq 11 to

$$\Delta \Phi_{\text{mem,e.c.}} = E_1^{\circ} + \frac{1}{2} R T F^{-1} \ln \left[ \mathbf{2}_{\text{ox}} \right]$$
 (12)

The small dependence of  $\Delta \Phi_{\text{mem,e.c.}}$  on [2<sub>ox</sub>] results from the logarithmic dependence of  $\Delta \Phi_{\text{mem,e.c.}}$  on [2<sub>ox</sub>] as well as the inclusion of ½ into the prelogarithmic term ½  $R T F^{-1}$ .

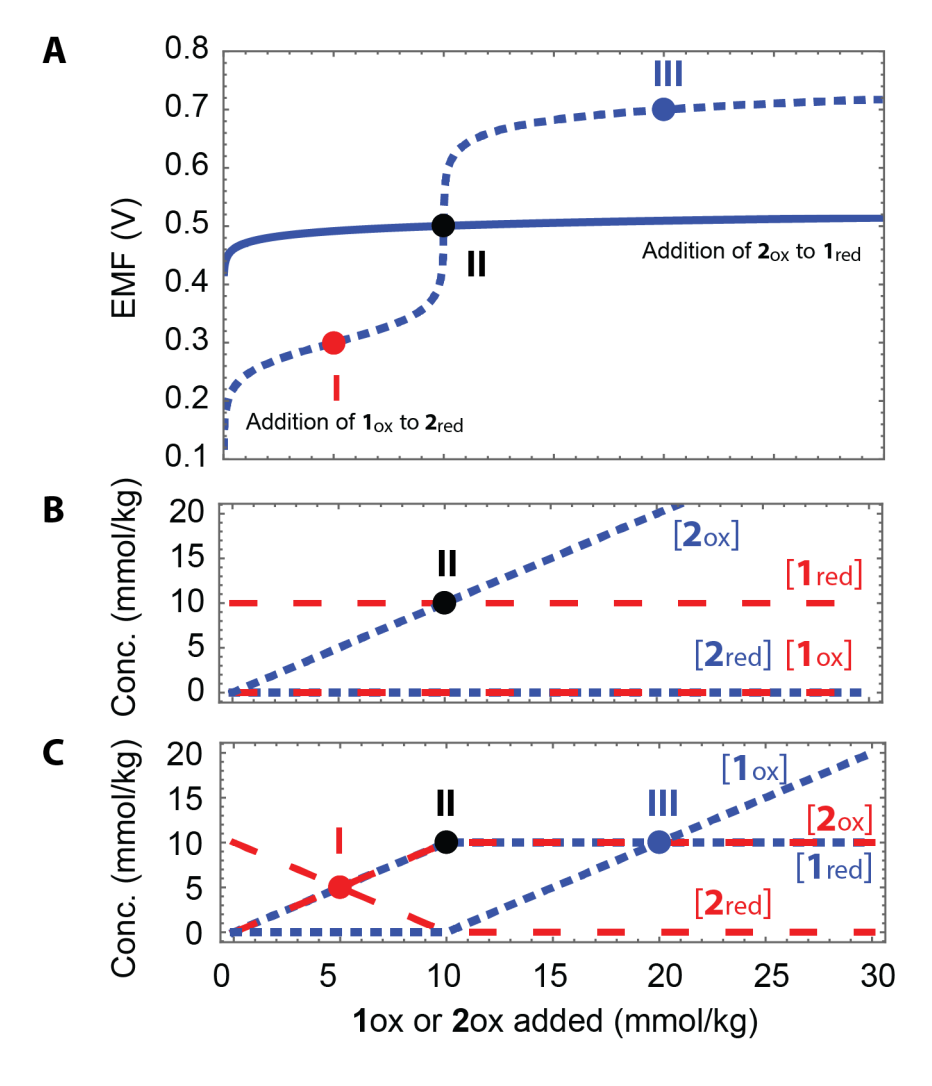


Figure 1. (A) Comparison of the potential arising from the addition of  $\mathbf{2}_{ox}$  to a solution of  $\mathbf{1}_{red}$  (10 mmol/kg, solid line) and a redox titration (dashed line) in which  $\mathbf{1}_{ox}$  is added to a solution of

 $\mathbf{2}_{\text{red}}$  (10 mmol/kg) for  $E_1^{\circ} = 0.7$  V,  $E_2^{\circ} = 0.3$  V,  $n_1 = n_2 = 1$ , and T = 298 K. (B) Species concentrations in the system corresponding to the solid line in Panel A. (C) Species concentrations corresponding to the redox titration shown as dashed line in Panel A.

Interestingly, the chemical composition of a system prepared from equal amounts of  $\mathbf{1}_{\text{red}}$  and  $\mathbf{2}_{\text{ox}}$  (with  $E_1^{\circ} >> E_2^{\circ}$ ) is identical with the chemical composition at the equivalence point of a redox titration of  $\mathbf{2}_{\text{red}}$  with  $\mathbf{1}_{\text{ox}}$ . This equivalence point is highlighted in Figure 1A with a black circle (point II). The change in potential for the corresponding redox titration is shown with a dashed line. (The Supporting Information shows the lengthy equation S12, which describes the shape of the redox titration curve and its derivation.) Note that for  $n_1 = n_2 = 1$ , the potential at point II is given by

$$\Delta \Phi_{\text{mem,e.c.}} = (E_1^{\circ} + E_2^{\circ}) / 2$$
 (13)

This relationship is well known to those familiar with redox titrations. Its proof is provided in the Supporting Information.

Evidently, near point II, the titration curve and the curve describing  $\Delta \Phi_{\text{mem,e.c.}}$  in a system prepared from  $\mathbf{1}_{\text{red}}$  and  $\mathbf{2}_{\text{ox}}$  could not differ more. While the former curve is nearly vertical, the latter is almost horizontal. The reasons for this dissimilarity are evident from Figures 1B and 1C, which illustrate the composition of the redox-active species as either  $\mathbf{2}_{\text{ox}}$  is added into a system containing  $\mathbf{1}_{\text{red}}$  at a constant concentration (Figure 1B), or as  $\mathbf{1}_{\text{ox}}$  is added to a solution of  $\mathbf{2}_{\text{red}}$  in a redox titration (Figure 1C). In the latter case, prior to the equivalence point, both  $\mathbf{2}_{\text{ox}}$  and  $\mathbf{2}_{\text{red}}$  are present in substantial concentrations, which is characteristic for a good redox buffer. The smallest slope of the titration curve (marked in Figures 1A and 1C with a red circle, point I) is half way to the equivalence point and occurs at  $\Delta \Phi_{\text{mem,e.c.}} = E_2^\circ$ . Beyond the equivalence point,

both  $\mathbf{1}_{ox}$  and  $\mathbf{1}_{red}$  are present in substantial concentrations. After addition of two equivalents of  $\mathbf{1}_{ox}$ , the potential reaches  $E_1^{\circ}$  (marked in Figures 1A and 1C with a blue circle, point III). Near the equivalence point, large potential changes are observed because either  $\mathbf{2}_{red}$  vanishes as a dominant species (before the equivalence point) or  $\mathbf{1}_{ox}$  appears as a new species that contributes to a new redox buffer (after the equivalence point).

The situation is very different for the addition of  $\mathbf{2}_{ox}$  to a system containing a constant concentration of  $\mathbf{1}_{red}$ . Despite the surprisingly small dependence of  $\Delta \Phi_{mem,e.c.}$  on  $[\mathbf{2}_{ox}]$ , this system never exhibits the characteristic of a conventional redox buffer, i.e., the presence of substantial concentrations of either  $\mathbf{1}_{ox}$  and  $\mathbf{1}_{red}$  or  $\mathbf{2}_{ox}$  and  $\mathbf{2}_{red}$ . Both  $\mathbf{1}_{ox}$  and  $\mathbf{2}_{red}$  have very low concentrations for any ratio of  $\mathbf{2}_{ox}$  and  $\mathbf{1}_{red}$ , as shown in Figure 1B.

Importantly, Figure 1A illustrates how  $\Delta \Phi_{\text{mem,e.c.}}$  for a system prepared with  $\mathbf{2}_{\text{ox}}$  and  $\mathbf{1}_{\text{red}}$  is affected by (i) weighing or dispensing errors, (ii) impurities of the reagents providing for  $\mathbf{2}_{\text{ox}}$  and  $\mathbf{1}_{\text{red}}$ , and (iii) redox-active interferents reacting with  $\mathbf{2}_{\text{ox}}$  or  $\mathbf{1}_{\text{red}}$  to give  $\mathbf{2}_{\text{red}}$  or  $\mathbf{1}_{\text{ox}}$ , respectively.

On one hand, for a constant concentration of  $\mathbf{2}_{ox}$ , any error resulting in a slightly lower or slightly higher concentration of  $\mathbf{1}_{red}$  will have only a miniscule effect on  $\Delta \Phi_{mem,e.c.}$ , as illustrated by the near flatness of the solid line at point II in Figure 1A. The same can be said about the dependence of  $\Delta \Phi_{mem,e.c.}$  on  $\mathbf{2}_{ox}$ . For the example illustrated in Figure 1 ( $E_1^{\circ} - E_2^{\circ} = 400 \text{ mV}$ ), to achieve a change in  $\Delta \Phi_{mem,e.c.}$  as small as 2 mV, an excess of 17% of  $\mathbf{2}_{ox}$  is needed. This provides  $\Delta \Phi_{mem,e.c.}$  with a remarkable robustness towards weighing errors or contamination of the reagents  $\mathbf{2}_{ox}$  or  $\mathbf{1}_{red}$  with redox-inactive impurities.

On the other hand, the value of  $\Delta \Phi_{\text{mem,e.c.}}$  of a system designed to contain only  $\mathbf{2}_{ox}$  and  $\mathbf{1}_{red}$  is exceptionally sensitive to small concentrations of  $\mathbf{2}_{red}$  and  $\mathbf{1}_{ox}$ , introduced either as impurities of the reagents for  $\mathbf{2}_{ox}$  and  $\mathbf{1}_{red}$  or resulting from other compounds that either oxidize  $\mathbf{2}_{ox}$  or reduce

 $1_{\text{red}}$ . If such impurities are present, the concentration of  $2_{\text{ox}}$  or  $1_{\text{red}}$  increases, and  $\Delta \Phi_{\text{mem,e.c.}}$  follows the characteristics of a poorly balanced redox buffer of the type  $2_{\text{ox}}/2_{\text{red}}$  or  $1_{\text{ox}}/1_{\text{red}}$ , as illustrated in Figure 1A by the steep increase of the dashed (titration) curve around the equivalence point (point II). The sensitivity of  $\Delta \Phi_{\text{mem,e.c.}}$  to  $2_{\text{red}}$  and  $1_{\text{ox}}$  (which are species that are not introduced into the system intentionally) is exceptional. For the example shown in Figure 1 ( $E_1^* - E_2^* = 400 \text{ mV}$ ), an excess of as little as 0.0065% of  $2_{\text{red}}$  will result in a change in  $\Delta \Phi_{\text{mem,e.c.}}$  of 2 mV. For a difference in the  $E^0$  values for  $2_{\text{ox}}/2_{\text{red}}$  and  $1_{\text{ox}}/1_{\text{red}}$  of 400 mV, this makes  $\Delta \Phi_{\text{mem,e.c.}}$  for the system consisting of  $2_{\text{ox}}$  and  $1_{\text{red}}$  more than three orders of magnitude more sensitive to impurities of  $2_{\text{red}}$  and  $1_{\text{ox}}$  than to impurities of  $2_{\text{ox}}$  and  $1_{\text{red}}$ . Indeed, the lack of non-potentiometric methods for the measurement of ppm level impurities of  $2_{\text{red}}$  and  $1_{\text{ox}}$  in samples of  $2_{\text{ox}}$  and  $1_{\text{red}}$  makes it extremely difficult to explain any  $\Delta \Phi_{\text{mem,e.c.}}$  values close to the equivalence point (i.e.,  $\Delta \Phi_{\text{mem,e.c.}} = \frac{1}{2}$  ( $E_1^* + E_2^*$ ) ) on the basis of independently measured or otherwise controlled values of  $[2_{\text{ox}}]$ ,  $[2_{\text{red}}]$ ,  $[1_{\text{ox}}]$ , and  $[1_{\text{red}}]$ .

# **EXPERIMENTAL SECTION**

# Materials

1-Octanethiol and 2,2'-bipyridine (bipy) were purchased from Alfa Aesar (Tewksbury, MA) and 4,4'-dinonyl-2,2'-bipyridyl (C<sub>9</sub>,C<sub>9</sub>-bipy) from TCI (Cambridge, MA). Lithium tetrakis(pentafluorophenyl)borate ethyl etherate (LiTPFPB) was purchased from Gelest (Morrisville, PA) and tributylmethylammonium bis(trifluoromethylsulfonyl)imide (MeNBu<sub>3</sub> TFSI) from IoLiTec (Tuscaloosa, AL). High molecular weight poly(vinyl chloride) (PVC), 2-nitrophenyl octyl ether (*o*-NPOE), potassium tetrakis(4-chlorophenyl)borate (KTClPB), and

tetradodecylammonium tetrakis(4-chlorophenyl)borate (ETH500) were purchased from Sigma Aldrich (St. Louis, MO). Gold disk electrodes (2 mm diameter) were purchased from CH Instruments (Austin, TX) and platinum microelectrodes (10 µm diameter) from BASi (West Lafayette, IN). Deionized water (0.18 M $\Omega$  m specific resistance) was obtained by purification with a Milli-Q PLUS reagent grade water system (Millipore, Bedford, MA). The tetrakis(pentafluorophenyl)borate salts of cobalt(II) tris(2,2'-bipyridyl), [Co(II)(bipy)<sub>3</sub>(TPFPB)<sub>2</sub>]; cobalt(III) tris(2,2'-bipyridyl), [Co(III)(bipy)<sub>3</sub>(TPPFB)<sub>3</sub>]; iron(II) tris(2,2'-bipyridyl), [Fe(II)(bipy)<sub>3</sub>(TPFPB)<sub>2</sub>]; osmium(II) tris(2,2'-bipyridyl), [Os(II)(bipy)<sub>3</sub>(TPFPB)<sub>2</sub>]; ruthenium(II) tris(2,2'-bipyridyl), [Ru(II)(bipy)<sub>3</sub>(TPFPB)<sub>2</sub>]; and cobalt(III) tris(4,4'-dinonyl-2,2'-bipyridyl), [Co(III)(C<sub>9</sub>,C<sub>9</sub>-bipy)<sub>3</sub>(TPFPB)<sub>3</sub>], were synthesized according to the literature with some modifications (see the Supporting Information for details).42,45,46

### Electrode Fabrication

The 2 mm diameter gold disk electrodes were polished over polishing cloths with aqueous dispersions of alumina (0.3 and 0.05  $\mu$ m), cleaned by ultrasonication in water and ethanol, and then dried with a flow of nitrogen. Afterwards, the electrodes were immersed into a 1.0 mM solution of 1-octanethiol in ethanol for 5 h to allow the formation of a self-assembled monolayer (SAM) of 1-octanethiol on the gold surface, which prevents the formation of a water layer between the ion-selective membrane and the gold surface.

The ion-selective membrane cocktail was prepared by dissolving 33 mg PVC (polymer matrix), 66 mg *o*-NPOE (plasticizer), 0.34 mg KTClPB (ionic sites), and varying amounts of redox-active organometallic complexes in 0.5 mL anhydrous tetrahydrofuran. Next, 40 µL of this solution was drop-cast onto a gold electrode modified with 1-octanethiol, which was then left to

dry for 24 h before use. Four types of ion-selective membranes were prepared by incorporating four different pairs of redox-active complexes, i.e., Co(II)(bipy)<sub>3</sub>(TPFPB)<sub>2</sub> and Co(III)(bipy)<sub>3</sub>(TPPFB)<sub>3</sub>, Fe(II)(bipy)<sub>3</sub>(TPFPB)<sub>2</sub> and Co(III)(C<sub>9</sub>,C<sub>9</sub>-bipy)<sub>3</sub>(TPFPB)<sub>3</sub>, Os(II)(bipy)<sub>3</sub>(TPFPB)<sub>2</sub> and Co(III)(C<sub>9</sub>,C<sub>9</sub>-bipy)<sub>3</sub>(TPFPB)<sub>3</sub>, and Ru(II)(bipy)<sub>3</sub>(TPFPB)<sub>2</sub> and  $Co(III)(C_9, C_9-bipy)_3(TPFPB)_3$ . Note that  $[Co(III)(C_9, C_9-bipy)]_3^{3+}$ , rather than  $[Co(III)(bipy)]_3^{3+}$ , was used to pair with the Ru(II), Fe(II) or Os(II) complex because its purity was found to be superior to that of [Co(III)(bipy)]<sub>3</sub><sup>3+</sup>. As shown by H NMR spectra (see Figures S2 and S3), the  $[Co(III)(C_{9},C_{9}-bipy)]_{3}^{3+}$  was found to be free of any observable impurities of the Co(II) complex,  $[Co(II)(C_9,C_9-bipy)]_3^{2+}$ , while extensive efforts to purify the  $[Co(III)(bipy)]_3^{3+}$  salt failed to remove an impurity of approximately 7 mol% of the [Co(II)(bipy)]<sub>3</sub><sup>2+</sup> salt. This value was taken into account for the calculation of correct Co(II)/Co(III) complex mole ratios, as reported in Table 2 and Figure 2.

For each type of membrane, three different mole ratios of the reduced and oxidized complexes were used, i.e., approximately 2 and 14 mmol/kg, 7 and 7 mmol/kg, and 14 and 2 mmol/kg. For control experiments, ion-selective membranes containing 7 mmol/kg of a single redox-active complex, i.e, Ru(II)(bipy)<sub>3</sub>(TPFPB)<sub>2</sub>, Fe(II)(bipy)<sub>3</sub>(TPFPB)<sub>2</sub>, Os(II)(bipy)<sub>3</sub>(TPFPB)<sub>2</sub> or Co(III)(C<sub>9</sub>,C<sub>9</sub>-bipy)<sub>3</sub>(TPFPB)<sub>3</sub>, were prepared. Ion-selective membranes that contained no redox-active organometallic complexes were also prepared and deposited onto bare, thiol-modified, and Au<sub>2</sub>O<sub>3</sub>-modified gold electrodes, respectively.

# Cyclic Voltammetry

Cyclic voltammograms (CVs) were obtained with a CHI660C potentiostat (CH Instruments, Austin, TX) with a scan rate of 0.1 V/s. A three-electrode set up was used with a gold disk macroelectrode or a platinum microelectrode as the working electrode, a Ag wire in 10 mM

AgNO<sub>3</sub> acetonitrile solution as the reference electrode (with a porous glass frit<sup>17,18</sup> to separate the sample from the AgNO<sub>3</sub> solution), and a platinum or gold wire as the counter electrode. For CVs measured with the gold disk macroelectrode, samples were prepared by dissolving 1.0 mM of a metal complex and 10 mM of ETH500 (as electrolyte) in *o*-NPOE. For CVs measured with the platinum microelectrode, samples were prepared by dissolving 1.0 mM of a metal complex and 100 mM of MeNBu<sub>3</sub> TFSI (as electrolyte) in *o*-NPOE.

#### Potentiometric Measurements

Potentials were measured with an EMF 16 potentiometer (input impedance 10 TΩ) controlled with EMF Suite 1.03 software (Lawson Labs, Malvern, PA). A free-flowing double-junction type external reference electrode<sup>49</sup> (DX200, Mettler Toledo, Switzerland; 3.0 M KCl saturated with AgCl as inner filling solution and 1.0 M LiOAc as bridge electrolyte) was used. Activity coefficients were calculated according to a two-parameter Debye–Hückel approximation,<sup>50</sup> and all emf values were corrected for liquid-junction potentials with the Henderson equation.

#### RESULTS AND DISCUSSION

# Control of the Phase Boundary Potential Across the Membrane-Metal Interface

The most direct evidence confirming that a redox couple controls the phase boundary potential at the interface of an ion-selective membrane to the underlying gold electrode comes from the dependence of the measured emf on the concentration ratio of the reduced and oxidized species, [red] / [ox], of that redox couple:

$$E_{cell}^{\circ} = E_{\text{const}} - R T F^{-1} \ln ([\text{red}] / [\text{ox}])$$
 (14)

Here,  $E_{cell}^{o}$  refers to the potential of the ISE cell as obtained by extrapolation of the linear section of the emf response to the activity of the measured ion in the aqueous sample to 1.0 M. The term  $E_{o}$  not only comprises the standard reduction potential of the redox couple in the ion-selective membrane (see, e.g., eqs 7 and 8), but it also includes the half cell potential of the reference electrode as well as the phase boundary potential across the interface of the aqueous sample and the ion-selective membrane.

Experimental evidence of this type has been previously reported for ISE membranes doped with the redox couple consisting of the Co(III) and Co(II) complexes of 1,10-phenanthroline.<sup>41</sup> It is shown here in Figure 2 for the redox couple consisting of the Co(III) and Co(II) complexes of 2,2'-bipyridine. This confirms that the electron transfer between these cobalt complexes and the underlying gold electrode is fast with respect to the timescale of potentiometric experiments. Evidently, the self-assembled monolayer of 1-octanethiol on the gold electrode (which inhibits the formation of a water layer between the ISE membrane and gold) does not slow down the electron transfer kinetics enough to prevent reversibility at this timescale. This is consistent with the fast electron transfer kinetics of the tris(4,4'-dinony1-2,2'-bipyridyl) Co(III)/Co(II) couple, as observed by us previously using cyclic voltammetry with SAM-modified gold electrodes.<sup>42</sup>

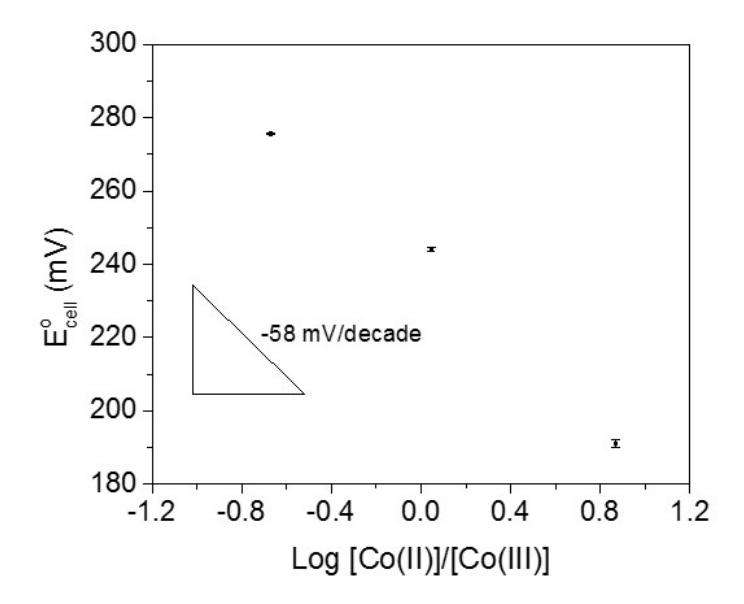


**Figure 2.** Dependence of  $E_{cell}^{\circ}$  on the ratio of  $Co(II)(bipy)_3(TPFPB)_2$  and  $Co(III)(bipy)_3(TPPFB)_3$ . Error bars refer to the standard deviation (n = 3 or 4, see Table 2).

In this work, ion-selective membranes were doped not only with Co(III) and Co(III) complexes but also with the analogous complexes [Fe(II)(bipy)<sub>3</sub>]<sup>2+</sup>, [Os(II)(bipy)<sub>3</sub>]<sup>2+</sup>, and [Ru(II)(bipy)<sub>3</sub>]<sup>2+</sup>. As reported in the literature, 51-53 standard electron transfer rate constants for these three complexes are more than five orders of magnitudes larger than for the corresponding cobalt complexes, which is consistent with fast electron transfer kinetics from these Fe(II), Os(II), and Ru(II) complexes to gold electrodes underlying ion-selective membranes doped with these compounds.

To confirm fast electron transfer kinetics for  $[Fe(II)(bipy)_3]^{2+}$ ,  $[Os(II)(bipy)_3]^{2+}$ , and  $[Ru(II)(bipy)_3]^{2+}$  in a medium relevant to this work, we performed cyclic voltammetry with the solvent o-NPOE, which was the PVC plasticizer used for all the potentiometric experiments reported here. Because o-NPOE has a viscosity that is an order of magnitude higher than water,<sup>54</sup> the diffusion coefficients of these complexes in o-NPOE are relatively small (see Figures S7 and

S8, Supporting Information). Consequently, the CVs measured with 10  $\mu$ m microelectrodes represent a convolution of both linear and spherical diffusion. The differences in  $E^{\circ}$  between the four complexes (see Table S1) agree within 0.05 V with values observed by Leddy and coworkers for Nafion films doped with the same type of complexes.<sup>51</sup> Importantly, the small peak separation for experiments with  $[Co(II)(bipy)_3]^{2+}$ ,  $[Fe(II)(bipy)_3]^{2+}$ ,  $[Os(II)(bipy)_3]^{2+}$ , and  $[Ru(II)(bipy)_3]^{2+}$  confirms fast electron transfer kinetics in o-NPOE (see Table S1, Supporting Information). The CVs also show that the  $E^{\circ}$  value for the  $[Co(II)(bipy)]_3^{2+}$  /  $[Co(III)(bipy)]_3^{3+}$  couple is only 0.05 V more negative than for the  $[Co(II)(C_9,C_9-bipy)]_3^{2+}$  /  $[Co(III)(C_9,C_9-bipy)]_3^{3+}$  couple, a small difference that seems consistent with the weakly electron-donating character of the six alkyl groups on the bipyridine ligands (see Figure S7).

# $E_{cell}^{\circ}$ for Membranes Doped with Different Organometallic Complexes

Jaworska and co-workers reported a very high reproducibility of  $E_{cell}^{"}$  for solid-contact ISEs comprising membranes doped with a Co(II) porphyrin and a Co(III) corrole." Specifically, for membranes with an equimolar ratio of the Co(II) porphyrin and Co(III) corrole complexes, a reproducibility of  $E_{cell}^{"}$  of  $\pm 0.7$  mV was observed for four sensors prepared the same way. No theoretical explanation was offered for this remarkable result, but at first sight, this finding appears to be consistent with the discussion presented here. In particular, the nearly horizontal solid line shown in Figure 1A for a system comprising  $\mathbf{1}_{\text{red}}$  and  $\mathbf{2}_{\text{ox}}$  (but neither  $\mathbf{1}_{\text{ox}}$  nor  $\mathbf{2}_{\text{red}}$ ) suggests that  $E_{cell}^{"}$  for a system comprising the Co(II) porphyrin / Co(III) corrole pair would show a very low sensitivity to minor changes in the Co(II) and Co(III) complex concentrations. Strong evidence for the beneficial effect of the Co(II) porphyrin / Co(III) corrole pair was also reported by the absence of oxygen interference on the measured emf for membranes doped with the

Co(II) porphyrin / Co(III) corrole pair, as opposed to a drift of approximately 80 mV in response to oxygen for membranes not doped with the Co(II) porphyrin / Co(III) corrole pair. As intriguing and provocative those results were, they were lacking evidence that *both* redox-active complexes influenced the observed  $E_{cell}^{o}$ . Jaworska et al. argued that use of the Co(II) porphyrin / Co(III) corrole pair resulted in a mixed potential, but no attempt was made to explain by theory the robustness of this mixed potential to redox-active impurities or minor variations in sensor fabrication.

To this end, we systematically studied solid-contact ISEs comprising membranes doped with either only [Ru(II)(bipy)<sub>3</sub>]<sup>2+</sup>, [Fe(II)(bipy)<sub>3</sub>]<sup>2+</sup>, [Os(II)(bipy)<sub>3</sub>]<sup>2+</sup>, or [Co(III)(C<sub>9</sub>,C<sub>9</sub>-bipy)]<sub>3</sub><sup>3+</sup> (see Table 1), or any of these three complexes in combination with [Co(III)(C<sub>9</sub>,C<sub>9</sub>-bipy)]<sub>3</sub><sup>3+</sup> in varying ratios (see Table 2). For comparison, the response of ISE membranes without added redox-active complexes were also tested (see Table 3). In all cases, the ion-selective membrane contained, besides the redox-active compounds, KTClPB to provide cation exchanger sites, *o*-NPOE as plasticizer, and PVC as polymer. To assure that the electrodes were fully functional, the response of these ISEs to the activity of K<sup>+</sup> in the aqueous sample was determined. As shown in Tables 1 to 3, all tested electrodes exhibited Nernstian slopes to K<sup>+</sup>, as expected for effective ISEs.

**Table 1.**  $E_{cell}^{\circ}$  and Response Slopes of ISE Membranes Containing 7 mmol/kg of  $[Ru(II)(bipy)_3]^{2+}$ ,  $[Fe(II)(bipy)_3]^{2+}$ ,  $[Os(II)(bipy)_3]^{2+}$ , or  $[Co(II)(C_9,C_9-bipy)]_3^{3+}$  in the Form of a TPFPB<sup>-</sup> Salt, KTClPB to Provide Cation Exchanger Sites, o-NPOE as Plasticizer, and PVC as Polymer.

Complex	$E_{cell}^{\circ}$ (mV)	Slope (mV/decade)	Number of ISEs
[Ru(II)(bipy) <sub>3</sub> ] <sup>2+</sup>	$186.3 \pm 7.9$	$59.9 \pm 0.4$	5
$[Fe(II)(bipy)_3]^{2+}$	$217.6 \pm 16.6$	$59.5 \pm 1.3$	4
[Os(II)(bipy) <sub>3</sub> ] <sup>2+</sup>	$221.6 \pm 11.3$	$62.2 \pm 0.3$	4
[Co(III) (C <sub>9</sub> ,C <sub>9</sub> -bipy) <sub>3</sub> ] <sup>3+</sup>	$132.5 \pm 1.7$	$59.6 \pm 0.5$	6

**Table 2.**  $E_{cell}^{\circ}$  and Response Slopes of ISE Membranes Containing [Ru(II)(bipy)<sub>3</sub>]<sup>2+</sup>, [Fe(II)(bipy)<sub>3</sub>]<sup>2+</sup>, [Os(II)(bipy)<sub>3</sub>]<sup>2+</sup>, or [Co(II)(bipy)]<sub>3</sub><sup>2+</sup> in Various Ratios to [Co(III)(C<sub>9</sub>,C<sub>9</sub>-bipy)]<sub>3</sub><sup>3+</sup> or [Co(III)(bipy)]<sub>3</sub><sup>3+</sup> in the Form of a TPFPB<sup>-</sup> Salt, KTClPB to Provide Cation Exchanger Sites, o-NPOE as Plasticizer, and PVC as Polymer.

Type of Complexes	Concentration Ratio (Number of Electrodes)	$E_{cell}^{\circ}$ (mV)	Slope (mV/decade)
$[Ru(II)(bipy)_3]^{2+}$	6.46 (n=3)	$192.8 \pm 2.3$	$61.3 \pm 0.1$
&	0.95 (n=4)	$149.4 \pm 1.3$	$60.3 \pm 0.2$
$[Co(III) (C_9,C_9-bipy)_3]^{3+}$	0.15 (n=4)	$142.0 \pm 1.8$	$59.5 \pm 0.5$
[Fe(II)(bipy) <sub>3</sub> ] <sup>2+</sup>	6.50 (n=3)	230.1 ± 1.5	$57.2 \pm 0.3$
&	0.87 (n=4)	$219.4 \pm 2.5$	$58.5 \pm 0.6$
$[Co(III) (C_9, C_9-bipy)_3]^{3+}$	0.14 (n=3)	$221.5 \pm 4.0$	$57.9 \pm 0.2$
[Os(II)(bipy) <sub>3</sub> ] <sup>2+</sup>	6.83 (n=3)	$190.1 \pm 1.0$	$59.4 \pm 0.3$
&	1.06 (n=4)	$211.7 \pm 2.5$	$60.3 \pm 0.3$
$[Co(III) (C_9,C_9-bipy)_3]^{3+}$	0.13 (n=3)	$217.6 \pm 1.3$	$59.2 \pm 1.7$
[Co(II) (bipy) <sub>3</sub> ] <sup>2+</sup>	7.37 (n=4)	190.0 ± 1.1	$59.0 \pm 0.2$
&	1.11 (n=3)	$244.1 \pm 0.6$	$59.1 \pm 0.1$
$[Co(III) (bipy)_3]^{3+}$	0.21 (n=3)	$275.6 \pm 0.2$	$59.9 \pm 0.2$

**Table 3.**  $E_{cell}^{\circ}$  and Response Slopes of ISE Membranes in Contact with Differently Prepared Gold Electrodes , KTClPB to Provide Cation Exchanger Sites, o-NPOE as Plasticizer, and PVC as Polymer.

Type of Au Electrode	$E_{cell}^{\circ}$ (mV)	Slope (mV/decade)	Number of ISEs
Thiolated <sup>a</sup>	$198.5 \pm 28.2$	$60.5 \pm 1.4$	5
$\mathrm{Au_2O_3}^{b}$	$251.2 \pm 23.8$	$60.4 \pm 0.8$	4
Bare Au <sup>c</sup>	$260.5 \pm 26.2$	$60.2 \pm 2.7$	4

<sup>&</sup>lt;sup>a</sup> Modified with a 1-octanethiol SAM by immersion for 5 h into a 1 mM solution of the thiol. <sup>b</sup> Prepared by immersion into 0.1 M H<sub>2</sub>SO<sub>4</sub> and 25 CV cycles between −0.155 and +1.545 V vs AgCl/Cl<sup>-</sup> with a scan rate of 0.1 V/s. <sup>c</sup> Polished, cleaned with hot piranha solution (1:3 mixture of 30% hydrogen peroxide and concentrated sulfuric acid), and rinsed with copious amounts of pure water. *Caution: piranha solution is highly oxidizing and should never be stored in closed containers*.

Surprisingly, a high reproducibility of  $E_{cell}^{\circ}$  within approximately 2 mV was observed for all twelve electrode types that contained  $[Ru(II)(bipy)_3]^{2+}$ ,  $[Fe(II)(bipy)_3]^{2+}$ ,  $[Os(II)(bipy)_3]^{2+}$ , or  $[Co(III)(bipy)]_3^{2+}$  in combination with  $[Co(III)(C_{\circ},C_{\circ}-bipy)]_3^{3+}$  or  $[Co(III)(bipy)]_3^{3+}$  (see Table 2), as it was similarly observed by Jaworska and co-workers for the Co(II) porphyrin / Co(III) corrole pair. However, the data is not consistent with systems comprising  $\mathbf{1}_{red}$  and  $\mathbf{2}_{ox}$  but neither  $\mathbf{1}_{ox}$  nor  $\mathbf{2}_{red}$ , as described in the Theory Section. A phase boundary potential at the membrane/gold interface that is well controlled by the redox-active species is only evident in the redox buffer

consisting of [Co(II)(bipy)]<sub>3</sub><sup>2+</sup> and [Co(III)(bipy)]<sub>3</sub><sup>3+</sup>, which is also represented by Figure 2. Interpolation of the theoretical slope of  $E_{cell}^{\circ}$  to the  $[Co(II)(bipy)]_3^{2+}$  /  $[Co(III)(bipy)]_3^{3+}$  ratio of 1 gives 241.3 mV. This value is the sum of the half cell potential of the reference electrode, the phase boundary potential at the sample/membrane interface, and a phase boundary potential at the membrane/gold interface corresponding to the formal reduction potential of the  $[Co(III)(bipy)]_3^{2+}$  /  $[Co(II)(bipy)]_3^{3+}$  couple in the membrane phase. Because the  $[Ru(III)(bipy)_3]^{3+}/[Ru(II)(bipy)_3]^{2+}, [Fe(III)(bipy)_3]^{3+}/[Fe(II)(bipy)_3]^{2+}, and [Os(III)(bipy)_3]^{3+}/[Fe(III)(bipy)_5]^{4+}/[Fe(III)(bipy)_5]^{4+}/[Fe(III)(bipy)_5]^{4+}/[Fe(III)(bipy)_5]^{4+}/[Fe(III)(bipy)_5]^{4+}/[Fe(III)(bipy)_5]^{4+}/[Fe(III)(bipy)_5]^{4+}/[Fe(III)(bipy)_5$ [Os(II)(bipy)<sub>3</sub>]<sup>2+</sup> couples all have reduction potentials that are 400 to 900 mV more positive than the [Co(III)(bipy)]<sub>3</sub><sup>2+</sup> / [Co(II)(bipy)]<sub>3</sub><sup>3+</sup> couple (as evident from the CV experiments; see Table S1, Supporting Information), it follows from eq 13 that  $E_{cell}^{\circ}$  for all combinations of  $[Ru(II)(bipy)_3]^{2+}$ ,  $[Fe(II)(bipy)_3]^{2+}$ , or  $[Os(II)(bipy)_3]^{2+}$  with  $[Co(III)(C_9,C_9-bipy)]_3^{3+}$  should be a few hundred millivolts positive of 241.3 mV. As shown by Table 2, this is clearly not the case. Instead,  $E_{cell}^{\circ}$  is for all twelve membrane formulations remarkably close to the values observed for the  $[Co(III)(bipy)]_3^{3+}$  /  $[Co(II)(bipy)]_3^{3+}$  couple. This shows that the species  $[Ru(II)(bipy)_3]_2^{2+}$ ,  $[Fe(II)(bipy)_3]^{2+}$ , and  $[Os(II)(bipy)_3]^{2+}$  do not control  $E_{cell}^{\circ}$  as predicted by eq 13. It also suggests that in the current work [Co(III)(C<sub>9</sub>,C<sub>9</sub>-bipy)]<sub>3</sub><sup>3+</sup> along with minor impurities of [Co(II)(C<sub>9</sub>,C<sub>9</sub>-bipy)]<sub>3</sub><sup>3+</sup> bipy)] $_3^{2+}$  dominated  $\Delta \Phi_{\text{mem,e.c.}}$ , and thereby  $E_{cell}^{\circ}$ , when the attempt was made to prepare membranes consisting of  $[Co(III)(C_9,C_9-bipy)]_3^{3+}$  and  $[Ru(II)(bipy)_3]^{2+}$ ,  $[Fe(II)(bipy)_3]^{2+}$ , or [Os(II)(bipy)<sub>3</sub>]<sup>2+</sup>. As shown in the Theory Section, even minute concentrations of redox-active impurities can shift  $\Delta \Phi_{\text{mem,e.c.}}$  away from the value of  $(E_1^{\circ} + E_2^{\circ})/2$  (i.e., the equivalence point) towards  $E_2^{\circ}$ , i.e., in this case the  $E^{\circ}$  of the  $[Co(III)(C_9,C_9-bipy)]_3^{2+}$  /  $[Co(II)(C_9,C_9-bipy)]_3^{3+}$ couple. This is consistent with the observation that the reproducibility of  $E_{\it cell}^{^{o}}$  for membranes

prepared with the [Co(III) (C<sub>9</sub>,C<sub>9</sub>-bipy)<sub>3</sub>]<sup>3+</sup> salt alone was, with  $\pm$  1.7 mV, remarkably good (Table 1). Apparently, because of this [Co(II)(C<sub>9</sub>,C<sub>9</sub>-bipy)]<sub>3</sub><sup>2+</sup> impurity, those membranes had a redox buffer capacity that was sufficient to make  $E_{cell}^{"}$  very reproducible, even though elemental analysis and <sup>1</sup>H NMR spectroscopy, with their respective sensitivities, suggested the [Co(III) (C<sub>9</sub>,C<sub>9</sub>-bipy)<sub>3</sub>]<sup>3+</sup> salt to be of high purity. Note that redox-active impurities may not only originate as impurities of the organometallic complexes used to prepare the redox buffers. Alternatively, redox-active impurities in the other components of the sensing membrane (or of samples) may affect the ratio of the reduced and oxidized form of the organometallic complexes. Indeed, we previously observed good reproducibilities of  $E_{cell}^{"}$  for membranes doped with either 14.2 or 1.4 mmol/kg [Co(III)(C<sub>9</sub>,C<sub>9</sub>-bipy)]<sub>3</sub><sup>2+</sup> / [Co(II)(C<sub>9</sub>,C<sub>9</sub>-bipy)]<sub>3</sub><sup>3+</sup> redox buffer, each with a 1:1 ratio of Co(II)/Co(III), but  $E_{cell}^{"}$  was 20.0 mV lower for the lower concentration of the redox buffer. While such a small difference could result from an ionic strength effect, it would also be consistent with a redox-active impurity of the plasticizer, polymer, or ion exchanger site that reacted with [Co(III)(C<sub>9</sub>,C<sub>9</sub>-bipy)]<sub>3</sub><sup>3+</sup> to give [Co(II)(C<sub>9</sub>,C<sub>9</sub>-bipy)]<sub>3</sub><sup>2+</sup>.

Interestingly, the addition of the  $[Ru(II)(bipy)_3]^{2+}$ ,  $[Fe(II)(bipy)_3]^{2+}$ , or  $[Os(II)(bipy)_3]^{2+}$  salt to the membranes doped with  $[Co(III)(C_9,C_9-bipy)]_3^{3+}$  is not without any effect, though. While these M(II) metal complexes do not shift  $E_{cell}^{ov}$  as expected from theory for pure compounds, they all shift  $E_{cell}^{ov}$  by tens of millivolts in a poorly predictable manner, which may be due to redoxactive impurities in these M(II) reagents (despite the high level of purity suggested by the elemental analysis and  $^1H$  NMR spectra; see the Supporting Information) or modulation of the ionic strength in the ion-selective membrane.

Results from membranes prepared without a redox-active metal complex are also consistent with the interpretation that the  $[Co(III)(C_9,C_9-bipy)]_3^{3+}$  /  $[Co(II)(C_9,C_9-bipy)]_3^{2+}$  couple dominates the  $E_{cell}^{\circ}$  for ion-selective membranes doped with combinations of [Co(III)(C<sub>9</sub>,C<sub>9</sub>bipy)] $_3^{3+}$  and [Ru(II)(bipy) $_3$ ] $_2^{2+}$ , [Fe(II)(bipy) $_3$ ] $_2^{2+}$ , or [Os(II)(bipy) $_3$ ] $_2^{2+}$ . As Table 3 shows, the  $E_{cell}^{\circ \circ}$ values for ISEs with membranes that do not contain a redox-active metal complex depend to some extent on the pretreatment of the gold electrode, i.e., whether the electrode is modified with a 1-octanethiol SAM, whether it is electrochemically oxidized to have a Au<sub>2</sub>O<sub>3</sub> surface layer, or whether it is cleaned only with piranha solution. However, in all cases the standard deviation for the  $E_{cell}^{\circ}$  reproducibility is an order of magnitude higher than in the case of any system containing either  $[Co(III)(C_9,C_9-bipy)]_3^{3+}$  only, or both  $[Co(III)(bipy)]_3^{3+}$  and  $[Co(II)(bipy)]_3^{2+}$ . Moreover, use of membranes doped with [Ru(II)(bipy)<sub>3</sub>]<sup>2+</sup>, [Fe(II)(bipy)<sub>3</sub>]<sup>2+</sup>, or [Os(II)(bipy)<sub>3</sub>]<sup>2+</sup> but no Co(III) complex resulted in the same large standard deviation in  $E_{\it cell}^{\it o}$  values that are statistically not different from those for membranes without organometallic complex on an underlying gold electrode modified with a 1-octanethiol SAM. Evidently, in the absence of a Co(III) species,  $[Ru(II)(bipy)_3]^{2+}$ ,  $[Fe(II)(bipy)_3]^{2+}$ , and  $[Os(II)(bipy)_3]^{2+}$  have no effect on  $E_{cell}^{\circ}$ .

# **CONCLUSIONS**

As reported previously, redox buffers that contain equal concentrations of the oxidized and reduced species of a redox couple stabilize the phase boundary potential at the interface with an electron conductor to a value readily predictable with the Nernst equation. As expected for a good redox buffer, addition of moderate concentrations of oxidant or reductant have only minimal effects on this phase boundary potential. Surprisingly, as shown in this work, theory also predicts that the phase boundary potential at the interface of an electron conductor and a

mixture of an oxidized and a reduced species has only a minimal dependence on the ratio of the concentrations of the two species if those two species are not a redox couple. However, as also shown here, this prediction only applies when the oxidized and reduced species are completely pure in terms of their redox state, i.e., when the oxidized species is not partially reduced to the species with which it would form a redox couple, and when the reduced species is not partially oxidized to the species with which it would form a redox couple. In real life, this condition appears to be remarkably difficult to achieve as even very small impurities alter the phase boundary potential in the same drastic way as it is expected for the endpoint of a redox titration.

Our experimental results show a surprisingly good reproducibility of approximately 2 mV for a range of electrode types with solid contacts that were prepared to contain an oxidized and a reduced species that do not form a redox couple. This is consistent with a very similar result by Jaworska and co-workers for solid contacts comprising a Co(III) corrole / Co(II) porphyrin pair. However, in view of the theoretical discussion and experimental results presented here, this remarkable reproducibility of  $E_{cell}^{\circ}$  is unlikely the result of the presence of an oxidized and a reduced species that do not form a redox couple. Instead, it is more likely the result of a very small redox state impurity of one (or both) of the two redox-active compounds. Specifically, in our work, the  $[Co(III)(C_9,C_9-bipy)]_3^{3+}$  /  $[Co(II)(C_9,C_9-bipy)]_3^{2+}$  couple dominates  $E_{cell}^{\circ}$  for solid contacts prepared to contain  $[Co(III)(C_9,C_9-bipy)]_3^{3+}$  and  $[Ru(II)(bipy)_3]_2^{2+}$ ,  $[Fe(II)(bipy)_3]_2^{2+}$ , or  $[Os(II)(bipy)_3]_2^{2+}$ .

We conclude that solid contacts prepared to contain the reduced and oxidized form of a redox couple are still the preferred choice for calibration-free solid-contact ISEs. Considering the remarkable experimentally observed in-batch reproducibility of  $E_{cell}^{\circ}$ , it appears tempting to use ISEs with solid contacts prepared to contain only the reduced or the oxidized form of a redox

couple. However, since this remarkable reproducibility appears to be the result of redox state

impurities, it is very unlikely that that same high reproducibility still applies when ISEs are

stored for longer times, when different lots or alternative suppliers of the redox-active

compounds are used, or when measured samples contain redox-active components.

ASSOCIATED CONTENT

Supporting Information

Derivation of the equations required to compute redox titration curves as those shown in

Figure 1A and the species concentrations shown in Figure 1C. Synthesis of organometallic

complexes. CVs of redox-active complexes.

**AUTHOR INFORMATION** 

Corresponding Author

\* Email: <u>buhlmann@umn.edu</u>

**ACKNOWLEDGMENT** 

This work was supported by the National Science Foundation (CHE-1748148). X.V.Z.

acknowledges a Lester C. and Joan M. Krogh Fellowship and C. R. R. acknowledges a Kenneth

E. & Marion S. Owens Endowed Fellowship, both from the Department of Chemistry,

University of Minnesota.

REFERENCES

(1) Bobacka, J.; Ivaska, A.; Lewenstam, A. Chem. Rev. 2008, 108, 329-351.

27

- (2) Amemiya, S. In *Handbook of Electrochemistry*; Zoski, C. G., Ed.; Elsevier: Amsterdam, 2007.
- (3) Bakker, E.; Pretsch, E. In *Electroanalytical Chemistry*; CRC Press: 2011, pp 1-74.
- (4) Bakker, E.; Bühlmann, P.; Pretsch, E. *Chem. Rev.* **1997**, 97, 3083-3132.
- (5) Bühlmann, P.; Pretsch, E.; Bakker, E. *Chem. Rev.* **1998**, *98*, 1593-1688.
- (6) Bühlmann, P.; Chen, L. D. In Supramol. Chem.; John Wiley & Sons, Ltd: 2012.
- (7) Lindner, E.; Gyurcsanyi, R. E. J. Solid State Electrochem. 2009, 13, 51-68.
- (8) Lewenstam, A. Electroanalysis 2014, 26, 1171-1181.
- (9) Lan, W. J.; Zou, X. U.; Hamedi, M. M.; Hu, J. B.; Parolo, C.; Maxwell, E. J.; Bühlmann, P.; Whitesides, G. M. Anal. Chem. 2014, 86, 9548-9553.
- (10) Ainla, A.; Mousavi, M. P. S.; Tsaloglou, M. N.; Redston, J.; Bell, J. G.; Fernandez-Abedul, M. T.; Whitesides, G. M. *Anal. Chem.* **2018**, *90*, 6240-6246.
- (11) Lugert-Thom, E. C.; Gladysz, J. A.; Rabai, J.; Bühlmann, P. *Electroanalysis* **2018**, *30*, 611-618.
- (12) Sokalski, T.; Ceresa, A.; Zwickl, T.; Pretsch, E. J. Am. Chem. Soc. **1997**, 119, 11347-11348.
- (13) Hu, J. B.; Stein, A.; Bühlmann, P. TrAC Trends Anal. Chem. 2016, 76, 102-114.
- (14) Lindfors, T.; Hofler, L.; Jagerszki, G.; Gyurcsanyi, R. E. Anal. Chem. 2011, 83, 4902-4908.
- (15) Chumbimuni-Torres, K. Y.; Rubinova, N.; Radu, A.; Kubota, L. T.; Bakker, E. *Anal. Chem.* **2006**, *78*, 1318-1322.
- (16) Veder, J. P.; De Marco, R.; Clarke, G.; Chester, R.; Nelson, A.; Prince, K.; Pretsch, E.; Bakkert, E. *Anal. Chem.* **2008**, *80*, 6731-6740.
- (17) Cattrall, R.; Freiser, H. Anal. Chem. 1971, 43, 1905-1906.
- (18) Cadogan, A.; Gao, Z.; Lewenstam, A.; Ivaska, A.; Diamond, D. *Anal. Chem.* **1992**, *64*, 2496-2501.
- (19) Bobacka, J. Anal. Chem. **1999**, 71, 4932-4937.
- (20) Bobacka, J. *Electroanalysis* **2006**, *18*, 7-18.
- (21) Kisiel, A.; Marcisz, H.; Michalska, A.; Maksymiuk, K. Analyst 2005, 130, 1655-1662.
- (22) Lindfors, T. J. Solid State Electrochem. 2009, 13, 77-89.
- (23) Walcarius, A.; Kuhn, A. *TrAC Trends Anal. Chem.* **2008**, 27, 593-603.
- (24) Yin, T.; Oin, W. TrAC Trends Anal. Chem. **2013**, *51*, 79-86.
- (25) Cuartero, M.; Bishop, J.; Walker, R.; Acres, R. G.; Bakker, E.; De Marco, R.; Crespo, G. A. Chem. Commun. **2016**, *52*, 9703-9706.
- (26) Lai, C.-Z.; Fierke, M. A.; Stein, A.; Bühlmann, P. Anal. Chem. 2007, 79, 4621-4626.
- (27) Fierke, M. A.; Lai, C.-Z.; Bühlmann, P.; Stein, A. Anal. Chem. **2010**, 82, 680-688.

- (28) Lai, C.-Z.; Joyer, M. M.; Fierke, M. A.; Petkovich, N. D.; Stein, A.; Bühlmann, P. J. Solid State Electrochem. 2009, 13, 123-128.
- (29) Crespo, G. A.; Macho, S.; Bobacka, J.; Rius, F. X. Anal. Chem. 2008, 81, 676-681.
- (30) Cuartero, M.; del Río, J. S.; Blondeau, P.; Ortuño, J. A.; Rius, F. X.; Andrade, F. J. *Anal. Chim. Acta* **2014**, 827, 95-102.
- (31) Hu, J.; Zou, X. U.; Stein, A.; Bühlmann, P. Anal. Chem. 2014, 86, 7111-7118.
- (32) Hu, J.; Ho, K. T.; Zou, X. U.; Smyrl, W. H.; Stein, A.; Bühlmann, P. Anal. Chem. **2015**, 87, 2981-2987.
- (33) Paczosa-Bator, B. Microchim. Acta 2014, 181, 1093-1099.
- (34) Hernández, R.; Riu, J.; Bobacka, J.; Vallés, C.; Jiménez, P.; Benito, A. M.; Maser, W. K.; Rius, F. X. *J. Phys. Chem. C* **2012**, *116*, 22570-22578.
- (35) Li, F.; Ye, J.; Zhou, M.; Gan, S.; Zhang, Q.; Han, D.; Niu, L. Analyst 2012, 137, 618-623.
- (36) Sun, Q.; Li, W.; Su, B. J. Electroanal. Chem. **2015**, 740, 21-27.
- (37) Bakker, E.; Bühlmann, P.; Pretsch, E. Talanta 2004, 63, 3-20.
- (38) Ishige, Y.; Klink, S.; Schuhmann, W. Angew. Chem., Int. Ed. 2016, 55, 4831-4835.
- (39) Klink, S.; Ishige, Y.; Schuhmann, W. ChemElectroChem 2017, 4, 490-494.
- (40) Liu, D.; Meruva, R. K.; Brown, R. B.; Meyerhoff, M. E. Anal. Chim. Acta 1996, 321, 173-183.
- (41) Zou, X. U.; Cheong, J. H.; Taitt, B. J.; Bühlmann, P. Anal. Chem. 2013, 85, 9350-9355.
- (42) Zou, X. U.; Zhen, X. V.; Cheong, J. H.; Bühlmann, P. Anal. Chem. **2014**, 86, 8687-8692.
- (43) Zou, X. U.; Chen, L. D.; Lai, C.-Z.; Bühlmann, P. *Electroanalysis* **2015**, 27, 602-608.
- (44) Jaworska, E.; Naitana, M. L.; Stelmach, E.; Pomarico, G.; Wojciechowski, M.; Bulska, E.; Maksymiuk, K.; Paolesse, R.; Michalska, A. *Anal. Chem.* **2017**, *89*, 7107-7114.
- (45) Yamaguchi, S.; Fukura, T.; Takiguchi, K.; Fujita, C.; Nishibori, M.; Teraoka, Y.; Yahiro, H. *Catalysis Today* **2015**, 242, 261-267.
- (46) Hung, M.; Stanbury, D. M. *Inorg. Chem.* **2005**, *44*, 9952-9960.
- (47) Mousavi, M. P. S.; Bühlmann, P. Anal. Chem. 2013, 85, 8895-8901.
- (48) Mousavi, M. P. S.; Saba, S. A.; Anderson, E. L.; Hillmyer, M. A.; Bühlmann, P. *Anal. Chem.* **2016**, *88*, 8706-8713.
- (49) Dohner, R. E.; Wegmann, D.; Morf, W. E.; Simon, W. Anal. Chem. 1986, 58, 2585-2589.
- (50) Meier, P. C. Anal. Chim. Acta 1982, 136, 363-368.
- (51) Gellett, W. L.; Knoche, K. L.; Rathuwadu, N. P.; Leddy, J. *J. Electrochem. Soc.* **2016**, *163*, H588-H597.
- (52) Young, R. C.; Keene, F. R.; Meyer, T. J. J. Am. Chem. Soc. 1977, 99, 2468-2473.
- (53) Doine, H.; Swaddle, T. W. Can. J. Chem. 1988, 66, 2763-2767.
- (54) Samec, Z.; Langmaier, J.; Trojánek, A. J. Electroanal. Chem. 1997, 426, 37-45.

# for TOC only

